A Mathematical Model characterising Achilles tendon dynamics in flexion

N. Chatzistefani*, M. J. Chappell*, C. Hutchinson, S. Kletzenbauer*** N. D. Evans***

**School of Engineering, University of Warwick, Coventry, CV4 7AL, United Kingdom (Tel:+442476573542; e-mail: N.Chatzistefani@warwick.ac.uk, e-mail: M.J.Chappell@warwick.ac.uk, e-mail: neil.evans@warwick.ac.uk).*

*** Population Evidence and Technologies, University Hospitals of Coventry and Warwickshire, Coventry, CV2 2DX, (e-mail: C.E.Hutchinson@warwick.ac.uk).*

****Ultrasound/Radiology Department, University Hospitals Coventry and Warwickshire, Coventry, CV2 2DX, (e-mail: Stephen.Kletzenbauer@uhcw.nhs.uk).*

Abstract: The purpose of this study is to acquire mechanistic knowledge of the gastrocnemius muscle-Achilles tendon complex behaviour during specific movements in humans through mathematical modelling. Analysis of this muscle-tendon complex was performed to see if already existing muscle-tendon models of other parts of the body could be applied to the leg muscles, especially the gastrocnemius muscle-Achilles tendon complex, and whether they could adequately characterise its behaviour. Five healthy volunteers were asked to take part in experiments where dorsiflexion and plantar flexion of the foot were studied. A model of the Achilles tendon-gastrocnemius muscle was developed, incorporating assumptions regarding the mechanical properties of the muscle fibres and the tendinous tissue in series. Ultrasound images of the volunteers, direct measurements and additional mathematical calculations were used to parameterise the model. Ground reaction forces, forces on specific joints and moments and angles for the ankle were obtained from a Vicon 3D motion capture system. Model validation was performed from the experimental data captured for each volunteer and from reconstruction of the movements of specific trajectories of the joints, muscles and tendons involved in those movements.

Keywords: Mathematical model, Hill-type muscle model, Muscle-tendon complex, Musculoskeletal modelling, Joint trajectories, Dorsiflexion, Plantar Flexion, Achilles tendon.

1. INTRODUCTION

The Achilles tendon is a fibrous tissue that connects the *plantaris*, *gastrocnemius* (calf) and *soleus* muscles of the lower leg to the *calcaneus bone* (heel) (Fig. 1). Its starting point is at the lower margins of the heads of the calf muscle and is located on the surface along almost the entire length of the *triceps surae* muscle (the soleus and gastrocnemius muscles) [1, 2].

Fig. 1. The Achilles tendon connects the heel to the calf and the soleus muscles of the leg (taken from [3] and used with permission of WebMD manager).

The Achilles tendon is the strongest and thickest tendon of the leg muscles and is crucial for normal propulsion and gait since its main role is to plantar flex the ankle [4]. When the calf muscles contract, they apply a force to the Achilles tendon and therefore push the foot downwards which results in walking, jumping, running, standing on toes, etc. [5]. Like other tendons, the Achilles tendon transmits tensile forces from the leg to the foot according to the amount of stretch it undergoes. Inversion of the heel, as well as plantar flexion, are produced by these forces when they pass through the ankle and the subtalar joints. Thus, movement in the subtalar joints and the ankle is created [6]. The mechanical properties of the Achilles tendon allow it to store and transmit elastic strain energy during fast locomotion and other movements [7]. That is why it is described as an energy-saving mechanism and a spring and shock absorber during gait [8]. It has been demonstrated through measurements of the mechanical properties of the Achilles tendon, that there is a variation in the elastic properties and the stiffness of the tendon between individuals [9, 10].

The Achilles tendon in the literature has been modelled as a straight line that begins near the middle of the calf and is inserted on the posterior part of the heel, or just as a single

point that is inserted into the middle part of the rear of the calcaneus bone. In order to define stress and strain in the Achilles tendon and acquire information about its loading during motion, mathematical models have been developed and experiments using the methods of ultrasound and motion capture have been used to directly measure tendon length changes during dynamic movements [6, 7, 11-13]. Yet, there is vast agreement between all authors that it is a very challenging task to model the Achilles tendon correctly due to the difficulties bestowed when representing its structure, material properties, kinetics and mechanisms.

In order to help in describing the Achilles tendon and its properties, motion capture and imaging were chosen as experimental methods in this study to assist in creating the actual geometry of the tendon and the muscle as well as re-enacting the changes in length of the Achilles tendon and the gastrocnemius muscle when in movement. Furthermore, the combination of the extension of existing foot and muscle models and the mathematical constructs of those models together with the incorporation of nonlinear spring characteristics were used in order to better characterise the gastrocnemius muscle-Achilles tendon complex. Previous muscle-tendon models that incorporate the gastrocnemius muscle usually include the Achilles tendon as a free tendon, but do not focus on the tendon properties. The innovation in this paper is that the focus of the muscle-tendon model lies on the Achilles tendon and its mechanistic behaviour. This is introduced in the following sections.

2. MATERIALS AND METHODS

2.1 Model of the Achilles tendon, the gastrocnemius muscle and the human foot

A two segment model of the human foot and leg was created in order to develop a musculoskeletal model of the Achilles tendon [14]. As presented in Fig. 2, it is comprised of i) the Achilles tendon connecting the heel and the gastrocnemius muscle, ii) the gastrocnemius muscle connecting to the Achilles tendon and the tibia, iii) the tibia originating from the ankle joint and ending at the knee and iv) the foot, that is represented by a triangle whose vertices are the heel, the ankle joint and the toe [14]. The foot in the literature is represented either as a rigid body or as two segments when the toe joint is included. For the purpose of the experiments, in this paper, it is being represented as rigid.

The ankle consist of three joints: the ankle joint, the subtalar joint, and the inferior tibiofibular joint. The ankle joint connecting the tibia (leg bone) to the talus (foot joint) has one degree of freedom and the movements produced at this joint are dorsiflexion and plantar flexion of the foot. The subtalar joint, which occurs at the meeting of the talus and the calcaneus, allows the inversion and eversion of the foot but plays no role in dorsiflexing or plantarflexing the foot and it also has one degree of freedom. The subtalar joint can also allow pronation and supination to occur which provides the third degree of freedom. Since the ankle joint is the dominant one in the foot segment, the subtalar joint was not incorporated in this study. Also the Achilles tendon plays part in the dorsiflexion and plantarflexion of the foot mostly. That is when it mostly shortens or lengthens and that is why these movements were selected to be analysed in this paper.

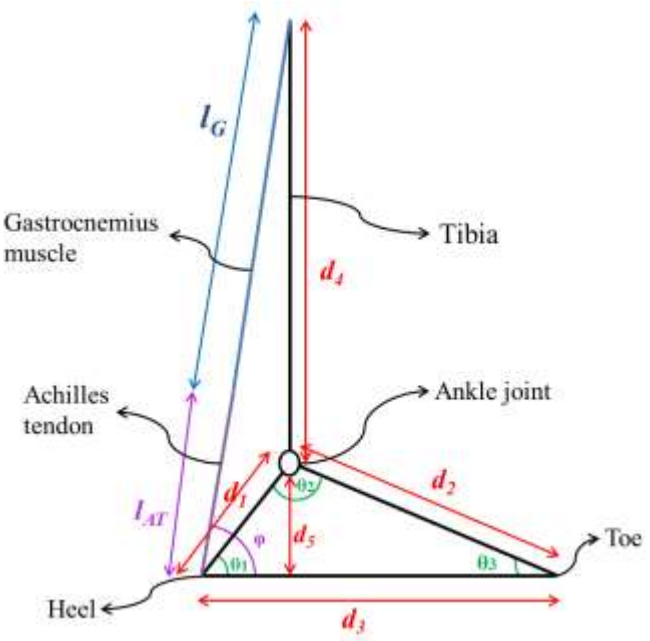

Fig. 2. Two segment model of the foot-leg illustrating the connection between the Achilles tendon, the gastrocnemius muscle, the heel and the tibia [14].

The lengths seen in Fig. 2 define the distances given in Table 1 and were determined by palpation and surface measurement of the legs of volunteers. All lengths were measured in mm, while the volunteers were standing still in an upright position so that the orientation of each segment would be exactly the same as the representation of the coordinate system, i.e. the normalised directions of the three axes in global space with reference to the force plate [15].

Table 1. Definition of distances

d_1 (mm)	the distance between the heel and the ankle joint
d_2 (mm)	the distance between the ankle joint and the toe
d_3 (mm)	the distance between the heel and the toe
d_4 (mm)	the length of the tibia
d_5 (mm)	the distance of the ankle from the floor
l_G (mm)	anatomical length of the gastrocnemius muscle
l_{AT} (mm)	anatomical length of the Achilles tendon

2.2 System equations

Knowledge of the patterns of the forces exerted by the gastrocnemius muscle on the Achilles tendon and vice versa is necessary in order to study the forces that the Achilles tendon transmits from the leg to the foot. Hence, it is crucial to calculate these forces indirectly using anthropometric and readily available kinematic data. The process by which the reaction forces and muscle moments are computed is called *link-segment modelling* [16, 17]. In order to calculate joint reaction forces and muscle moments we need to have full knowledge of the external forces applied to the joints, a kinematic description of the movement and accurate anthropometric measurements for each of the volunteers participating in the experiments. Using this two segment model and *inverse dynamics* it should be possible to predict any joint and tendon reactions needed [18].

Newton's second and third laws were used to derive the system equations for the musculoskeletal model of the Achilles tendon shown in Figs. 2, 3, 4 and 5. Figs. 2 and 3 portray the ankle joint dynamics when someone is standing still in an upright position, Fig. 4 when dorsiflexing their foot and Fig. 5 when plantar flexing their foot. As seen in Fig. 3 the foot is represented by a triangle whose vertices are the heel (H), the ankle joint (A) and the toe (T). All other references to the triangle in this paper will be referred to as triangle HTA.

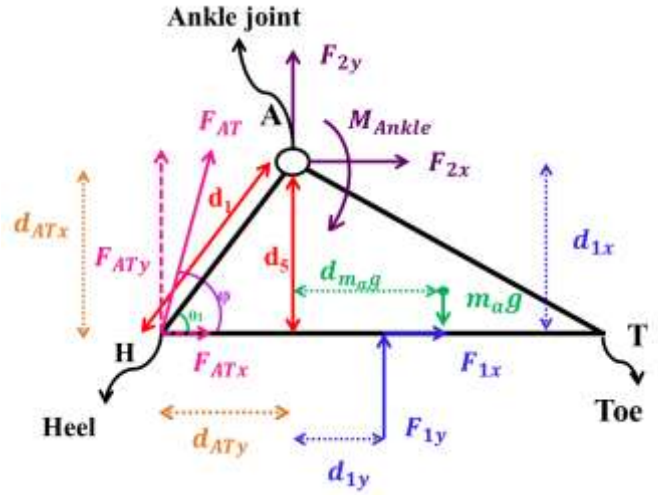

Fig. 3. Free body diagram of the foot segment during weight bearing in static position [14].

The equations describing a static trial (Fig. 3) are given by:

$$\sum F_x = 0 \Rightarrow \; F_{1x} + F_{2x} + F_{ATx} = 0 \tag{1}$$

$$\sum F_y = 0 \Rightarrow F_{1y} + F_{2y} + F_{ATy} - m_a g = 0 \tag{2}$$

$$M_{ankle} = F_{1x} d_{1x} + F_{1y} d_{1y} - m_a g d_{m_a g} + F_{ATx} d_{ATx} - F_{ATy} d_{ATy} \tag{3}$$

where the definition of the variables included in these equations are given in Table 2. The acceleration along both the *x* and *y* axes of the segment is 0 m/s^2 since during a static trial the volunteer does not move.

Table 2. Definition of variables for the static trial

x	subscript that represents the horizontal plane of action
y	subscript that represents the vertical plane of action
F (N)	force applied to the ankle joint or the heel depending on the subscripts
1	subscript that signifies the external ground reaction force
2	subscript that denotes the force acting on the foot at the ankle joint because of the tibia
AT	subscript that symbolises the Achilles tendon force acting on the foot at the heel
a	Subscript that represents the centre of the mass of the foot
m_ag (N)	force due to the mass of the foot under gravity
M_{ankle} (N mm)	moment at the ankle joint
d (mm)	distance of the ankle joint from the heel, the Achilles tendon and the centre of mass of the foot depending on the subscript
m (kg)	mass of the foot segment

The equations describing the dynamic trials of dorsiflexion and plantar flexion as seen in Fig.4 and 5 respectively are listed below.

$$\sum F_x = ma_x \Rightarrow F_{1x} + F_{2x} + F_{ATx} = ma_x \tag{4}$$

$$\sum F_y = ma_y \Rightarrow F_{1y} + F_{2y} + F_{ATy} - m_a g = ma_y \tag{5}$$

$$M_{ankle} = F_{1x} d_{1x} + F_{1y} d_{1y} + m_a g d_{m_a g} + F_{ATx} d_{ATx} + F_{ATy} d_{ATy} - I_0 \alpha \tag{6}$$

where the definition of the variables included in these equations are given in Table 3. The acceleration along the *x* and *y* axes of the segment is no longer 0 m/s^2 since the volunteer is moving. In Fig. 4 and 5 θ_1 is the angle between sides HT and HA of the triangle HTA and φ is the angle between the Achilles tendon and the sole of the foot. The force m_ag and its distance d_{m_ag} from the ankle joint found in equations (2), (3), (5) and (6) are calculated using the anthropometric data. This table provides the segment mass as a fraction of the body mass and the centres of mass as fractions

of the lengths of the segments. The angles in the triangle HTA and that of the Achilles tendon shown in Figs. 3, 4 and 5, are estimated from the coordinates of the markers placed on the ankle joint, the heel, the toe and the Achilles tendon during the experiments conducted in the University of Warwick Gait Laboratory. Also the moment of inertia about the ankle joint I_0 found in equation (6) is calculated from the anthropometric data in Table 4.1 from Winter. All calculations are based on the examples given in Winter on how to evaluate all the unknowns in equations (1)-(6) from experimental data taken from a motion capture system, such as Nexus as used in the experiments [16].

Table 3. Definition of variables for a dynamic trial

x	subscript that represents the horizontal plane of action
y	subscript that represents the vertical plane of action
F (N)	force applied to the ankle joint or the heel depending on the subscripts
1	subscript that signifies the distance between the level that F_{1x} and F_{1y} is applied and the ankle joint
2	subscript that denotes the distance between the level that F_{2x} and F_{2y} is applied and the ankle joint
AT	subscript that symbolises either the Achilles tendon force acting on the foot at the heel or the distance between the level that F_{ATx} and F_{ATy} is applied and the ankle joint depending on the superscript
$m_a g$ (N)	force due to the mass of the foot under gravity
a_x, a_y (mm/s^2)	acceleration of the foot segment in the horizontal and vertical plane of action respectively
α (rad/s^2)	angular acceleration of the foot segment
M_{ankle} (N mm)	moment at the ankle joint
d (mm)	distance of the ankle joint from the heel and the Achilles tendon depending on the subscript
$d_{m_a g}$ (mm)	distance calculated from the coordinates of the markers and table 4.1 from Winter [16]
I_0 (kg mm^2)	moment of inertia about the ankle joint calculated from the coordinates of the markers and table 4.1 from Winter [16]
m (kg)	mass of the foot segment

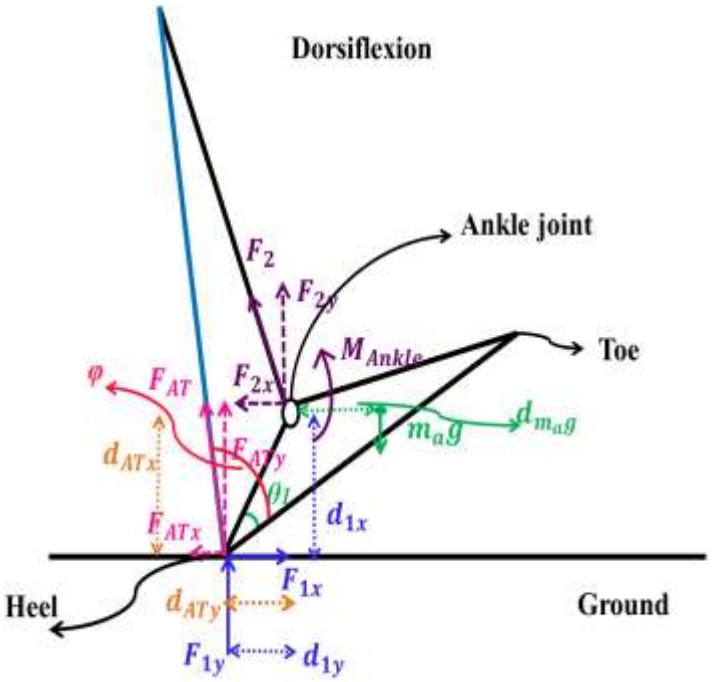

Fig. 4. Dorsiflexion of the foot [14].

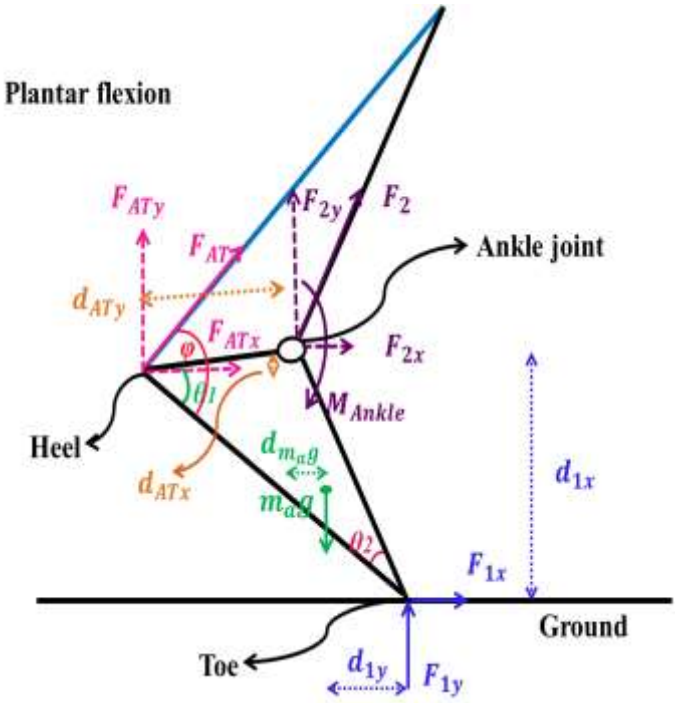

Fig. 5. Plantar flexion of the foot [14].

Using kinetic and kinematic Gait Laboratory data, equations (1)-(3) for the static trials and equations (4)-(6) for the dynamic trials, i.e. dorsiflexion and plantar flexion, are solved numerically and yield the Achilles tendon force F_{AT} that is then substituted into the muscle-tendon model in section 2.6 in

order to estimate the parameters of the model. Also displacements of the Achilles tendon and the gastrocnemius muscle for each movement are calculated from the trajectories of the markers and are coupled with the muscle-tendon displacements in section 2.6.

2.3 Muscles

Muscles perform four important functions for the body: they generate heat, stabilise joints, maintain posture of the body and produce movements. Skeletal muscles have natural resting lengths [16, 19-21]. Depending on internal and external forces applied to the skeleton, muscles can lengthen, shorten or remain constant. The part of the muscle that shortens and lengthens and that is responsible for generating force and tension in the muscle is the *contractile element*. The muscle components that are responsible for producing a contractile force are the actin and myosin filaments of the myofibrils within the muscle fibre cells. However, it is not possible to measure the dynamic properties of these components *in vivo* [22]. That is why parameter estimation techniques are used to obtain parameter values for our mathematical and mechanical models using the experimental data collected.

2.4 Hill-type Muscle Models

When describing and creating a muscle-tendon model, Hill-type muscle models are commonly used. In the early nineteen hundreds Hill developed a simple but widely accepted model of muscle function suitable for defining the basic mechanics of the muscles and for modelling specific beaviours of muscles during voluntary human movements [21, 23]. Since this early work, progress had been made towards the understanding of muscular structure and its function and new Hill-type muscle models have been created [24, 25].

In all Hill-type muscle models there is an *active* element, the *contractile element* (CE). The amount of the force the contractile element produces is determined by the mechanical characteristics of the element and can be represented by four relationships: stimulation-activation, force-activation, force-velocity and force-length [26]. The contractile element is enclosed by a *passive* element, a connective tissue that behaves as an elastic band and is called the *parallel elastic component* (PEC) [16]. The summation of the forces from both elements gives us the total muscle force-length characteristics [16, 26]. Since the early work by Hill, knowledge has grown on the *series elastic component* (SEC) that represents all the connective tissue in series with the CE including the tendon which in our case is the Achilles tendon. It is believed that these SECs store large amounts of energy as muscles stretch before an explosive shortening. In order to determine the force-length characteristics of the SEC, experiments that require dynamic changes of force or length on an isolated muscle are needed [16]. Thus in our analysis we studied the isometric (constant muscle length) and isotonic (constant force) contractions of the gastrocnemius muscle-Achilles tendon complex.

2.5 Gastrocnemius muscle-Achilles tendon complex analysis

A range of mechanical models of muscles - Crowe (1970)[27], Gottlieb and Agarwal (1971)[28], Winter (1995)[16], Haeufle (2014)[24] - exist that describe and calculate the tension of a muscle depending on different inputs. All of these use a modified Hill-type muscle model with different connections between the CE, the PEC and the SEC elements. Generally, Hill-type muscle models have as an input, muscle-tendon lengths, muscle-tendon contraction velocities or neural muscle stimulations and as an output a force that is usually applied between the insertion points and the origins of the muscle or tendon analysed. By simulating different movements of the muscles with these models, one can predict the passive and active muscle forces.

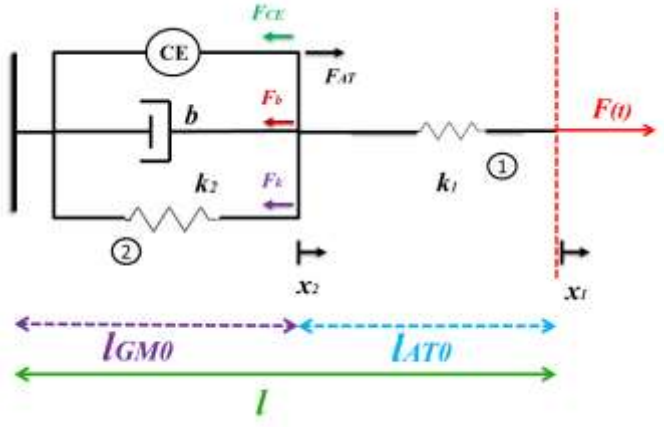

Fig. 6. Analysis of movement of the Modified Hill-type muscle model representing the gastrocnemius muscle-Achilles tendon complex.

As seen in Fig. 6, a modified Hill-type muscle model has been used to investigate the mechanical characteristics of the Achilles tendon and the gastrocnemius muscle. The gastrocnemius muscle is represented by: i) the contractile element (CE) that represents the force source when the muscle is activated, ii) the parallel damping element that is described by a damper where b (Ns/m) is the damping coefficient and denotes the ability of the muscle to resist its shortening or lengthening depending on the movement studied, and iii) the parallel elastic element (PEC) that is defined by the spring numbered as 2 with stiffness k_2 (N/m) that shows the ability of the gastrocnemius muscle to return to its natural resting length. A series elastic element k_1 shows the series elastic component (SEC) of the model and represents the behaviour of the Achilles tendon in the complex [7, 16, 22-24, 26, 29]. All other connective tissue was ignored since the Achilles tendon is the dominant tendon connecting the heel to the gastrocnemius muscle and the one that can be studied more accurately with the methods used in the associated experiments. The damping characteristic of the SEC is considered to be relatively small and does not influence the general behaviour of the model; that is why it is ignored in this study.

2.6 Response of the Active Muscle

The transfer function of the Hill-type muscle model seen in Fig. 6 can be used to find the active muscle response. A similar approach has been investigated for the muscles of the upper limb [26]. As seen in Fig. 6 the externally measured force F can be defined by the force of the contractile element F_{CE} that is changed by the force of the damping element F_b and that of the parallel elastic element F_k. The total force F is transferred through the series elastic element that represents the Achilles tendon whose force is denoted by F_{AT}, resulting in the following two equilibrium equations:

$$\vec{F} = \vec{F}_{CE} + \vec{F}_b + \vec{F}_k \tag{7}$$

$$\vec{F} = \vec{F}_{AT} . \tag{8}$$

Analysing the movement of the muscle-tendon complex in Fig. 6 gives the following equations where (9) and (10) are the system specific forms of (7) and (8) respectively:

$$F = F_{CE} - b\frac{dx_2}{dt} - k_2 x_2 \tag{9}$$

$$F = k_1 (x_2 - x_1)^{\alpha} \tag{10}$$

where α is a positive integer (α =1,2 or 3). If the spring element describing the Achilles tendon is considered to be linear then α equals 1 and if it is considered nonlinear then α equals 2 or 3. As mentioned in section 2.2 F_{AT} is calculated from experimental data and is substituted into the muscle-tendon model. For a static trial equations (1)-(3), and for a dynamic trial equations (4)-(6) are used to calculate the Achilles tendon force F_{AT}. F_{1x} and F_{1y} that compute the ground reaction force, F_{2x} and F_{2y} that represent the force on the ankle joint, a_x and a_y that give the acceleration of the foot segment and M_{ankle} that gives the moment at the ankle joint are provided directly from the Vicon Nexus system. All distances d_{1x}, d_{1y}, d_{2x}, d_{2y}, d_{ATx}, and d_{ATy} that are explained in Tables 2 and 3 are calculated from the coordinates of the markers placed on the feet of the volunteer provided by the Vicon Nexus system. As mentioned in section 2.2 $m_a g$ and $d_{m_a g}$ are calculated from Winter [16]. So the only unknown that is the force of the Achilles tendon is calculated. So the full set of the model equations is given by equations (1)-(3) and (4)-(6) with coupling of (9)-(10). Parameter estimation was performed in the time domain and is described in section 4.1. In order to validate the model qualitatively Laplace transforms of the model equations were used as described in the following part of this section.

Since the Achilles tendon is the dominant tendon that transmits the force from the heel (and the foot eventually) to the gastrocnemius muscle and vice versa and since no other external forces are applied to the muscle-tendon model, F is assumed to be equal to F_{AT} in equations (9) and (10). Initially we assume that the spring is linear (α=1). The displacement of the gastrocnemius muscle is denoted by x_2 and the displacement of the muscle-tendon complex is x_1 and is measured from the insertion point of the Achilles tendon to the heel which is the right end of spring 1. As mentioned previously, muscles and tendons have natural resting lengths when no force or stimulation is acting upon them. The natural lengths of the muscle and the Achilles tendon are denoted by l_{GM0} and l_{AT0} respectively. When in movement the length of the muscle and the tendon change and become $l_{GM}=l_{GM0}+x_2$ and $l_{AT}= l_{AT0}+x_1-x_2$ respectively. Displacements x_1 and x_2 (in mm) are calculated from the displacements measured from Gait Laboratory experiments. In more detail, l_{GM}, l_{GM0}, l_{AT} and l_{AT0} (in mm) are known from the displacements captured in the experiments and computed from equations (1)-(6).
Assuming zero initial conditions:

$$x_1(0) = x_2(0) = 0 . \tag{11}$$

Using equation (10) to replace x_2 in equation (9) and taking Laplace transforms gives:

$$F_{CE}(s) = \frac{k_1 + k_2 + bs}{k_1} F_{AT}(s) + (k_2 + bs) X_1(s) . \tag{12}$$

Equation (12) can be rearranged into two different forms. One is the equation that describes the external muscle force/tension F_{AT} as a function of the force produced by the active contractile element. Solving (12) for F_{AT} gives:

$$F_{AT}(s) = F_{CE}(s)\frac{k_1}{k_1 + k_2 + bs} - \frac{k_1(k_2 + bs)}{k_1 + k_2 + bs} X_1(s) . \tag{13}$$

The other is the expression of displacement X_1 in terms of the external force and the force from the contractile element of the active muscle. Solving (12) for X_1 gives:

$$X_1(s) = \frac{F_{CE}(s)}{(k_2 + bs)} - \frac{k_1 + k_2 + bs}{k_1(k_2 + bs)} F_{AT}(s) . \tag{14}$$

In order to validate the model qualitatively the following scenarios were investigated. In an isometric contraction, the muscle contracts without shortening considerably since both of its ends are strictly fixed so that it cannot shorten or lengthen. When the muscle is stimulated it contracts isometrically and the resulting external force can be measured experimentally [30, 31]. This scenario can be investigated using equation (13) where the second term is excluded, since no change in length, at least externally, is present. This means that x_1 equals zero but x_2 can be nonzero. Thus, (13) becomes:

$$F_{AT}(s) = F_{CE}(s)\frac{k_1}{k_1 + k_2 + bs} . \tag{15}$$

Assuming a maximum tetanic stimulation, where the muscle has been maximally stimulated and remains that way for some time, the input can be represented by a step function with magnitude of F_{CE}. Using the Laplace transform of the step function, equation (15) becomes:

$$F_{AT}(s) = F_{CE}\frac{k_1}{k_1 + k_2 + bs}\frac{1}{s} . \tag{16}$$

Taking the inverse Laplace transforms of (16) yields:

$$F_{AT}(t) = \frac{F_{CE} k_1}{k_1 + k_2} (1 - \mathrm{e}^{-\frac{k_1 + k_2}{b} t}). \quad (17)$$

Equation (17) takes the form of a step response of a first order linear system where the time constant is $b/(k_1+k_2)$ and the gain of the system is $k_1/(k_1+k_2)$. Nominal random values were used in Matlab 2016a to create a plot for equation (17) shown in Fig. 7. It resembles the build-up of tension measured in the isometric experiment of a tetanic stimulation of a muscle (Figure 4.12) in Freivalds [26]. Note that the force/tension (F_{CE}) of the contractile element when the muscle is activated, is amended by the combination of the parallel and series elastic elements that reduce its value. If the values of k_1 and k_2 are relatively equal, the force reduces to almost 50%. However, the values are not that close in the actual muscle, so the reduction is relatively small.

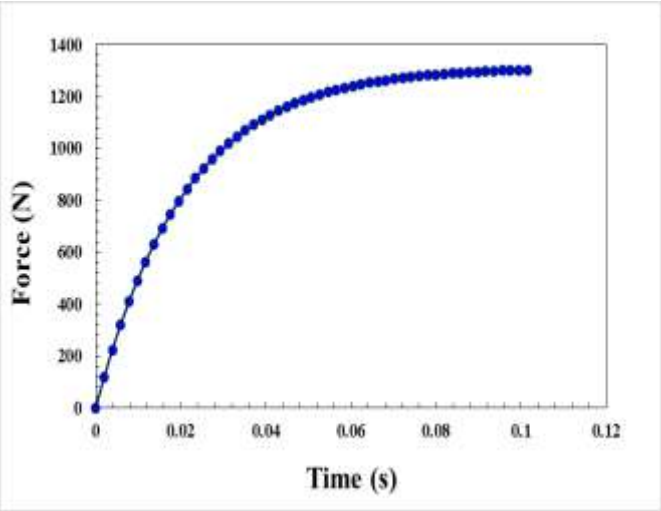

Fig. 7. Representation of the calculated force/tension over time that builds up when using the modified Hill-type muscle model.

Considering an isotonic contraction, tension develops to a point and then remains constant while the muscle changes its length. There are two types of isotonic contractions. The concentric contraction where the muscle shortens when its tension is greater than the force opposing it and the eccentric contraction, where the muscle elongates, lengthens when the force is greater than the muscle tension [26, 31, 32]. In the muscle-tendon complex studied, during isotonic contractions, the force exerted on the tendon is constant.

During isotonic contraction, the contractile element shortens, stretching the series elastic element before it develops tension so, for this case, its force F_{CE} is considered to be constant. For a purely passive movement F_{CE} is zero, hence the first term of equation (14) can be excluded yielding:

$$X_1(s) = -\frac{k_1 + k_2 + bs}{k_1(k_2 + bs)} F_{AT}(s). \quad (18)$$

Using a unit step input to describe the muscle-tendon tension, equation (18) transforms to:

$$X_1(s) = -\frac{k_1 + k_2 + bs}{k_1(k_2 + bs)} \frac{1}{s}. \quad (19)$$

Taking inverse Laplace transforms of (19) yields:

$$x_1(t) = -\frac{k_1 + k_2}{k_1 k_2} + \frac{e^{-\frac{k_2}{b} t}}{k_2}. \quad (20)$$

Nominal values were used in Matlab 2016a to simulate equation (20) shown in Fig. 8. In this scenario where a unit step input of force is applied and the contractile element stretches the series elastic element before it develops tension of its own. The damping element does not react initially. Still, the series elastic spring stretches and a step jump of movement is observed where the displacement of the muscle-tendon complex does not start from zero. Subsequently, the muscle continues to load and the damping element begins to yield until the two elastic springs balance out the force and the movement stabilises. The plot resembles the figure of the measured creep (the change in the displacement over time) in the isotonic experiment of the upper limb model (Figure 4.15) in Freivalds [26].

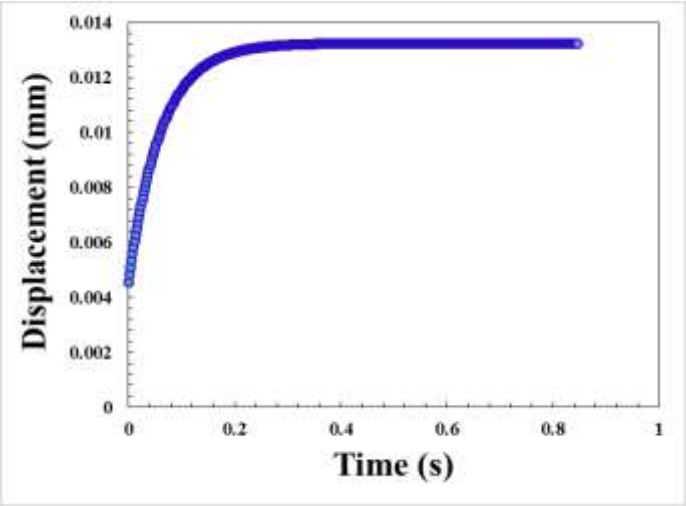

Fig. 8. Calculated displacement of the Hill-type muscle model versus time.

2.7 Structural Identifiability analysis of the gastrocnemius muscle-Achilles tendon model

Structural identifiability analysis should be performed when developing mathematical models, since it assists in determining whether parameters in a mathematical model can be uniquely identified or otherwise from the available observations. Parameters can be either globally identifiable, locally identifiable, or unidentifiable. Globally identifiable parameters are those that can be uniquely identified, locally identifiable are those that have a finite number of solutions and unidentifiable are those that have an infinite number of solutions.

Structural identifiability is defined as follows. Let the generic parameter vector $\boldsymbol{p}$ belong to a feasible parameter space $\boldsymbol{P}$ such that $\boldsymbol{p} \in \boldsymbol{P}$. Let $y(t, \boldsymbol{p})$ be the output function from the state-

space model. Further, consider a parameter vector $\bar{\boldsymbol{p}}$ where $y(t, \boldsymbol{p}) = y(t, \bar{\boldsymbol{p}})$ for all t. If this equality, in a neighbourhood $N \subset \boldsymbol{P}$ of $\boldsymbol{p}$, implies that $\boldsymbol{p} = \bar{\boldsymbol{p}}$ then the model is structurally locally identifiable. If $N = \boldsymbol{P}$ then the model is globally structurally identifiable. For a structurally unidentifiable parameter, p_i in $\boldsymbol{p}$, every neighbourhood N around $\boldsymbol{P}$ has a parameter vector $\bar{\boldsymbol{p}}$ where $p_i \neq \bar{p}_i$ that gives rise to identical input-output relations.

Before commencing the parameter estimation, structural identifiability analysis of the model should be taken into account as part of the experimental design process. In order to obtain unique parameter estimates when real data are available from experiments, a globally or at least locally identifiable model has to be defined. If the model is proven to be unidentifiable, then re-parameterisation techniques can be used to possibly give a locally identifiable model [32, 33]. The data used in the analysis are assumed to be perfect, i.e. continuous and noise free.

Equations (9) and (10) were studied in order to determine the structural identifiability of the parameters of the muscle-tendon model. For observations of x_1, x_2 and F_{CE} and for the linear case where a=1, the model parameters b, k_1, and k_2 are clearly structurally identifiable (by comparison of $y(t, \boldsymbol{p}) = y(t, \bar{\boldsymbol{p}})$.

3. EXPERIMENTAL METHODOLOGY

In order to validate the mathematical approach that was analysed in the previous sections, experiments were conducted at UHCW and the University of Warwick Gait Laboratory.

3.1 Imaging

In this study, ultrasound scans were provided by the University Hospitals of Coventry and Warwickshire (UHCW) in order to measure the changes in length of the Achilles tendon in dorsiflexion and plantar flexion of the foot segment so as to design and validate the gastrocnemius muscle-Achilles tendon complex [34, 35]. Ultrasound sessions were performed at the UHCW with volunteers from the University of Warwick. A sonographer scanned the Achilles tendons on both feet of the volunteers. He first scanned the volunteers lying still on a bed to measure the natural resting length, also named as anatomical length, of the Achilles tendon. Then the volunteers were asked to dorsiflex and plantar flex their feet to the maximum of their abilities and the total length of the Achilles tendon was scanned. All images obtained from UHCW and used for this study comply with NHS ethics approval for the collection and use of such images.

3.2 Participants

Five healthy volunteers from the University of Warwick took part in the experiments, after giving written informed consent. Two were male and three female, between the ages of 25 to 35 years, with body mass 81±10kg and body height 1.71±0.10m. None of them had experienced any Achilles tendon injuries or ruptures in the past or had any Achilles tendon pathologies. There were no other requirements of the participants apart from their ability to walk around a room for up to 10 minutes unaided. Ethical approval complying with the research code of practice of the University of Warwick had been granted for all the above mentioned Gait Laboratory sessions and Ultrasound sessions at UHCW by the University's Biomedical and Scientific Research Ethics Committee (BSREC full approval *Simulation of the Achilles tendon* REGO-2013-548AM01).

3.3 Experimental methodology

In order to acquire measurements for the parameters describing the muscle-tendon model and to validate the results, plantar flexion, dorsiflexion and human gait were studied. Gait analysis in general helps us study different kinds of movement patterns as well as the forces involved in producing those movements. Gait analysis is considered reliable since it uses computers and videography to capture, observe and interpret the different kinds of movements [36, 37].

The volunteers that participated in the Gait Laboratory sessions, the same as those that participated in the ultrasound sessions, were asked to stand still on a force plate, to dorsiflex and plantar flex their feet which means to flex and extend their feet at the ankle respectively.

The origin and insertion of the gastrocnemius muscle and the Achilles tendon were determined by palpating the legs of the participants before marker placement commenced and by using information from the ultrasound sessions that were performed on each volunteer before the Gait Laboratory sessions took place. The natural resting length of the Achilles tendon l_{AT0} as well as the change in its length during plantar flexion and dorsiflexion were measured directly from the ultrasound images obtained through the experiments at the UHCW. The origin and insertion point of the Achilles tendon were measured and marked for each volunteer in order to place the markers at the exact same positions when the same movements of resting, dorsiflexion and plantar flexion were studied in the Gait Laboratory. Movement of the skin at the site of the insertion of the Achilles tendon was found. The amplitude between the tendon insertion and the skin marker was measured in the direction of the tendon, and the average amplitude of skin movement across the range of movement was 5mm with a standard deviation of 2mm.

The natural resting length of the gastrocnemius muscle l_{G0} was determined by surface measurement and palpation of the legs of the subjects before placement of the markers. These lengths were then compared with those calculated from the coordinates of the markers placed at the origins of the Achilles tendon and the gastrocnemius muscle respectively (Vicon Nexus analysis). All lengths were measured in mm with measuring tape before the marker placement and compared with the calculated ones from the system after the marker placement. Since the gastrocnemius muscle is a curved surface, measuring its length with a measuring tape gives just an approximation that can be checked through ultrasound tests. The lengths of the gastrocnemius muscle for the mathematical model in section 2.2 and the muscle-tendon model in section 2.6 were calculated using data in Table 4.3 from Winter [16]. This table gives the mass, fibre length, physiologic cross-sectional area and pennation angle of some muscles of the human body including the gastrocnemius.

Vicon's three-dimensional (3D) biomechanical motion capture system was used to determine kinetics and kinematics of the foot in order to solve equations (1)-(6) for the Achilles tendon force and to solve equations (9)-(10) for the parameters b, k_1, and k_2.

4. RESULTS

4.1 Time Domain Model and Parameter estimation

Parameter estimation was performed in the time domain for each volunteer in order to acquire a set of fitted values for the parameters b, k_1, and k_2. Measured data of ankle and heel angle trajectories and Achilles tendon trajectories as well as gastrocnemius muscle trajectories were obtained from the experiments and were used to investigate the best fit for the parameters of the model, while simulated data were obtained from inverse dynamics created from equations (1)-(6) to determine model validation. As mentioned in 2.6 the values of x_2, (x_2-x_1) and dx_2/dt were calculated from the experimental data for each volunteer. The derivative term, dx_2/dt, was determined using the central difference formula:

$$\frac{dx_2(t_i)}{dt} = \frac{x_2(t_{i+1}) - x_2(t_{i-1})}{2\Delta t} \tag{21}$$

where t_i (i=1,2,…,N) are the sample times for a fixed time step Δt=t_{i+1}-t_i [16].

The curve fitting toolbox in Matlab 2016a was used in order to fit our experimental and simulated data. Equation (9) was used in order to find values for the parameters b and k_2 and equation (10) (for a=1) was used in order to find values for the parameter k_1. Custom equations were created to see which was the best fit for the dorsiflexion and plantarflexion experiments. The parameters b, k_1, and k_2 were constrained to be positive numbers and their confidence intervals are represented by the numbers in brackets under their values in Tables 4 and 5. A step input was found to appropriately describe the form of the force of the contractile element when the volunteers were dorsiflexing their feet. The residuals appeared random with no apparent pattern and the Root Mean Square Error (RMSE) for the best fit for each volunteer is presented in Table 4. Plantar flexion was found to be better defined by an impulsive input. The residuals appeared random with no apparent pattern and the RMSE for the best fit for each volunteer is presented in Table 5. All parameter values have a 95% confidence bound.

As seen in Tables 4 and 5 the values of the parameters b, k_1, and k_2 are different for each subject for dorsiflexion and plantar flexion of the foot. They have a similar orders of magnitude, but their values have differences that lie in the ranges of i) (0.005-0.015) (Ns/mm) for the damper element b, ii) (0.006-0.017) (N/mm) for the spring element of the Achilles tendon k_1 and iii) (0.06-0.4) (N/mm) for the spring element of the gastrocnemius muscle k_2. In plantarflexion, the primary muscles acting are the gastrocnemius, the soleus and plantaris muscles where the gastrocnemius is the most dominant and the only one that crosses both the ankle and the knee joint. In dorsiflexion, the most dominant muscle responsible for lifting the foot is the tibialis anterior that is located in the anterior part of the foot and is not connected with the Achilles tendon or the gastrocnemius or soleus muscle. This could be a reason for the differences in the values of the parameters b, k_1, and k_2 in dorsiflexion and plantar flexion.

Table 4. Values for the parameters b, k_1, and k_2 and their confidence intervals for each volunteer for dorsiflexion

Volunteer	***b*** **(Ns/mm)**	***k*₂ (N/mm)**	**RMSE**
1	0.0645 (0.057, 0.073)	0.099 (0.088, 0.111)	0.5245
2	0.0261 (0.0214, 0.031)	0.1322 (0.101, 0.125)	0.3059
3	0.0095 (0.0027, 0.016)	0.0543 (0.049, 0.059)	0.2284
4	0.0131 (0.0018, 0.024)	0.006 (0.0017,0.069)	0.1845
5	0.113 (0.1016, 0.124)	0.3206 (0.313, 0.328)	0.7257

Volunteer	***k*₁ (N/mm)**	**RMSE**
1	0.0893 (0.0881, 0.0905)	0.7203
2	0.1513 (0.1503, 0.1523)	0.3274
3	0.0644 (0.0642, 0.0647)	0.3093
4	0.1258 (0.1227, 0.1289)	1.234
5	0.1007 (0.0981, 0.1033)	1.402

In addition, a difference in the values of the parameters across the volunteers is observed. This is expected since the volunteers have different heights, body masses and different backgrounds e.g. in sports training. Volunteer 3 with the lowest values of the spring element k_1 and the lowest values of the damper element b in both dorsiflexion and plantar flexion had previously attended years of dance classes. Volunteers 1 and 5 that had the greatest body mass, appear to have the highest values of b in both dorsiflexion and plantarflexion which means that their gastrocnemius muscles have an ability to resist more when shortening or lengthening. However, since the sample of the volunteers is small, it is not possible to draw more generic conclusions for a general population.

Table 5. Values for the parameters b, k_1, and k_2 and their confidence intervals for each volunteer for plantarflexion

Volunteer	b (Ns/mm)	k_2 (N/mm)	RMSE
1	0.0494 (0.044, 0.0544)	0.1742 (0.1722, 0.1762)	0.5466
2	0.0149 (0.011, 0.0185)	0.2477 (0.2466, 0.2488)	0.1559
3	0.0127 (0.029, 0.0037)	0.1229 (0.1209, 0.1249)	0.3505
4	0.0207 (0.0008, 0.033)	0.4354 (0.4343, 0.4364)	0.136
5	0.1178 (0.1079, 0.127)	0.1751 (0.1701, 0.1801)	0.5235

Volunteer	k_1 (N/mm)	RMSE
1	0.1067 (0.106, 0.107)	0.2793
2	0.1623 (0.1613, 0.1633)	0.2542
3	0.0692 (0.06889, 0.0694)	0.1536
4	0.1536 (0.1498, 0.1573)	1.319
5	0.0943 (0.09233, 0.09626)	0.852

Following the parameter estimation, the values of the parameters b, k_1, and k_2 were used to plot the simulated data of the force for the Achilles tendon over time along with the experimental data of the Achilles tendon within the model (6)-(10) over time for each volunteer. An example plot of the simulated and experimental responses for volunteer 1 are given in Fig. 9.

The residuals for the simulated and measured Achilles tendon force data were also calculated and plotted for each volunteer. These appeared random in all cases with no apparent pattern. An example is shown in Fig. 10 where the residuals of the force data for the dorsiflexion of volunteer 1 are plotted for the whole movement.

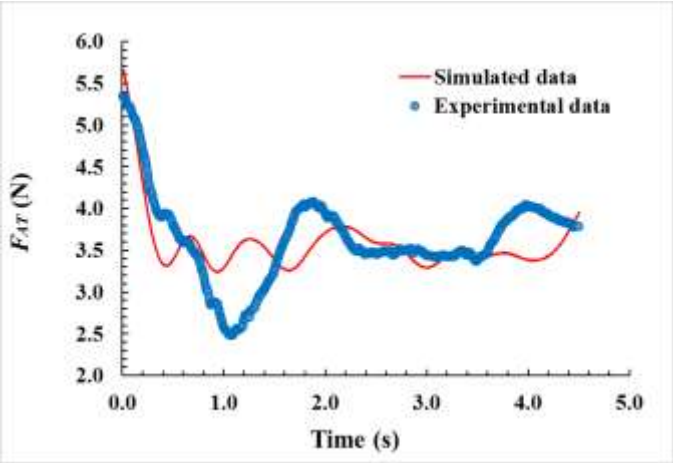

Fig. 9. Simulated and experimental data of the force of the Achilles tendon for volunteer 1 plotted over time.

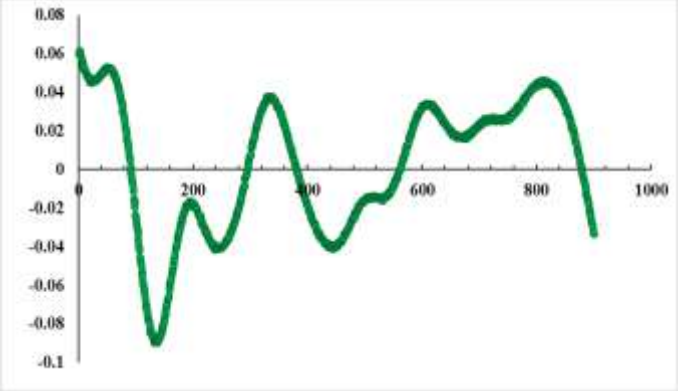

Fig. 10. Plotted residuals of the Achilles tendon force data for dorsiflexion for volunteer 1. The discrete points show the duration of the whole movement.

In addition, the displacements of the Achilles tendon over time were plotted. As seen in Figs. 11(a), (b), (c), (d) and (e) the simulated responses approach the measured data for each volunteer. The curve for displacement over time has a similar form for each volunteer when they are dorsiflexing their foot. Volunteers with similar heights as seen in Fig. 11 (a) and (e) have similar shapes of curves. The volunteer with the strongest background in sports/fitness training attains the highest maximum value of Achilles tendon displacement as seen in Fig. 11 (d). This was volunteer 4, who had the lowest value of parameter k_2 in dorsiflexion. A spring with a higher spring value needs more force to get the same amount of stretch than for a spring with lower spring value. Since the gastrocnemius muscle of volunteer 4 can shorten more with the same amount of force, his Achilles tendon can lengthen more and thus reach a maximum value of displacement that is larger than others.

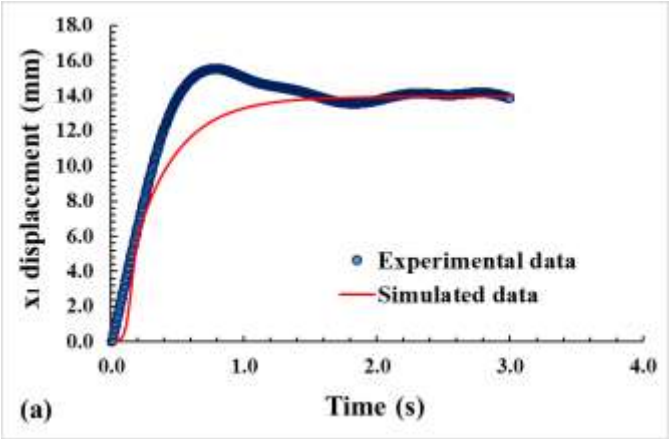

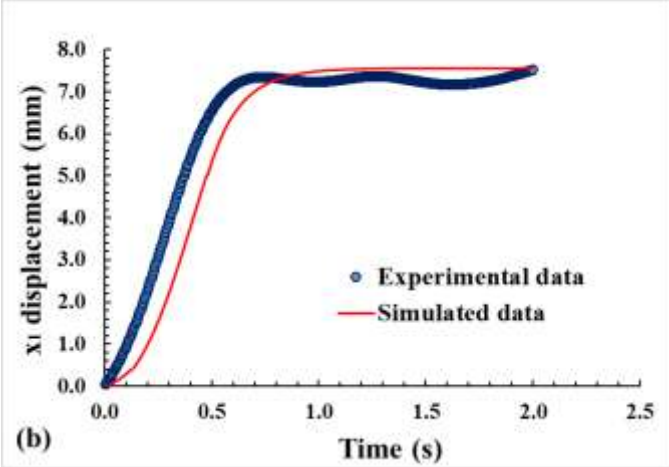

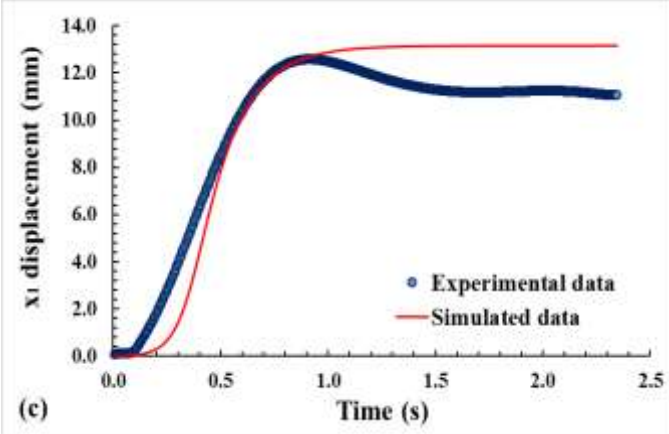

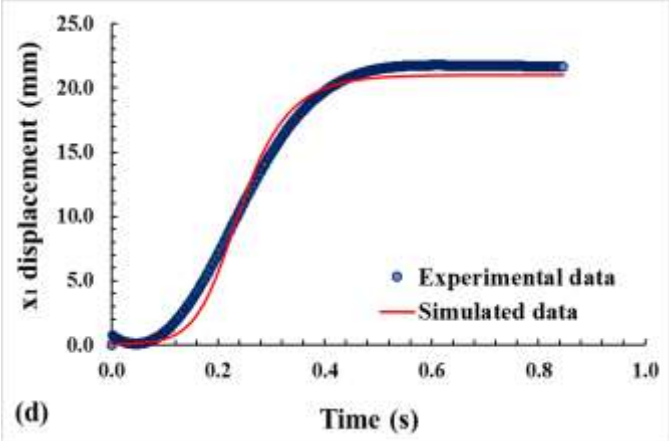

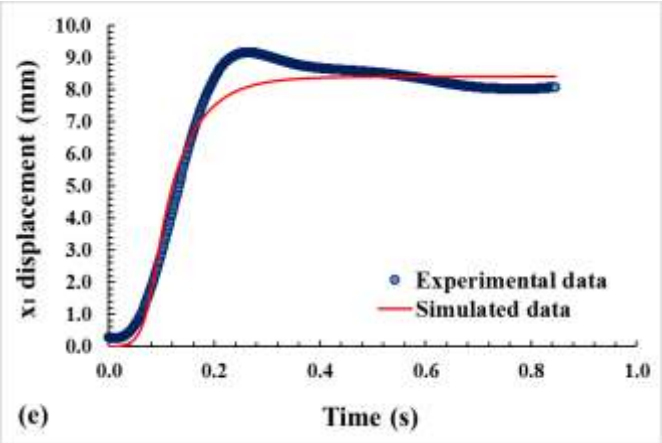

Fig. 11(a), (b), (c), (d), (e). Experimental and simulated data of the displacement of the Achilles tendon over time fitting the measured trajectories of the displacement over time of the Achilles tendon when dorsiflexion occurs for different volunteers.

4.2 Nonlinearity

As mentioned in section 2.6, nonlinear spring elements describing the Achilles tendon were also considered where α in equation (10) equals 2 and 3. These two cases were investigated to see if the nonlinear spring can describe the movement of the muscle-tendon complex in a more appropriate way. The solution of the system of equations (9) and (10) was studied where α in equation (10) equals 2:

$$F_{AT} = F_{CE} - b\frac{dx_2}{dt} - k_2 x_2 \text{ and } F_{AT} = k_1(x_2 - x_1)^2.$$

Solving the system of equations symbolically in Matlab 2016a gives:

$$x_2 = \frac{F_{CE} - F_{AT} + e^{-\frac{k_2}{b}t}(F_{AT} - F_{CE})}{k_2} \quad (22)$$

$$x_1 = x_2 + \frac{\sqrt{k_1 F_{AT}}}{k_1} \text{ or } x_1 = x_2 - \frac{\sqrt{k_1 F_{AT}}}{k_1} \quad (23)$$

where x_2 and x_1 are the displacements described in section 2.6 and seen in Fig. 6. In order to examine if these equations can explain any of the movements studied, different values for parameters b, k_1, and k_2 were applied and values for the forces F_{AT} and F_{CE} were used according to the data obtained from the experiments conducted. Fig. 12 illustrates plantar flexion of the foot of one volunteer, where the different curves are explained in the legend of the figure. As seen from the plot, the simulated data approach the experimental data when $x_1 = x_2 - \sqrt{(k_1 F_{AT})/k_1}$.

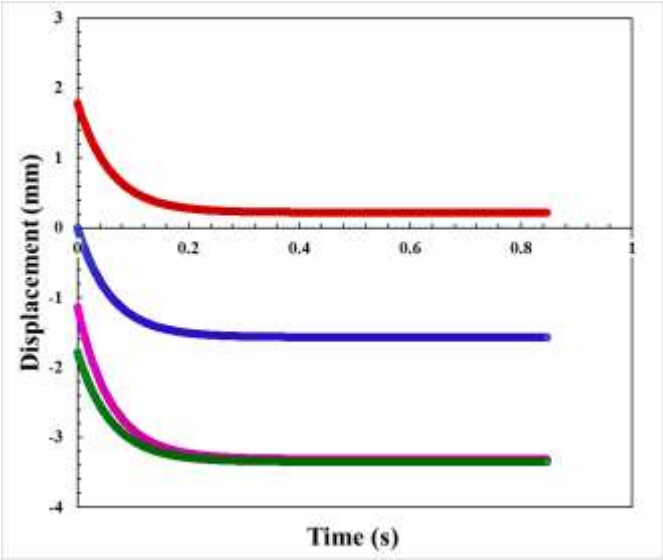

Fig. 12. Displacement over time when volunteer is plantar flexing foot. The blue line denotes the displacement x_2 over time. The magenta line symbolises the experimental data of the displacement of the muscle-tendon complex over time. The red line represents the simulated displacement of the complex when $x_1 = x_2 + \sqrt{(k_1 F_{AT})/k_1}$ over time and the green line presents the simulated displacement of the complex when $x_1 = x_2 - \sqrt{(k_1 F_{AT})/k_1}$ over time.

The solution of the following system of equations was also studied where a=3 in equation (10):

$$F_{AT} = F_{CE} - b\frac{dx_2}{dt} - k_2 x_2 \text{ and}$$

$$F_{AT} = k_1 x_2^{\,3} - 3k_1 x_2^{\,2} x_1 + 3k_1 x_2 x_1^{\,2} - k_1 x_1^{\,3}.$$

The analytical solutions were generated symbolically in Matlab 2016a and gave equation (24) as the solution of the ordinary differential equation:

$$x_2 = \frac{F_{CE} - F_{AT} + e^{-\frac{k_2}{b}t}(F_{AT} - F_{CE})}{k_2} \qquad (24)$$

and one real root and a complex conjugate pair of roots for the cubic equation. However, the mathematical solutions of the cubic equation for x_1 that are complex numbers cannot represent a displacement of a length. So further investigation was carried out only on the real root that is shown in (25):

$$x_1 = x_2 + C \text{, where } C = \left(-\frac{-k_1 x_2^3 + F_{AT}}{k_1} - x_2^3\right)^{1/3} \qquad (25)$$

As described above for the quadratic equation, different values for parameters b, k_1, and k_2 were applied and values for the forces F_{AT} and F_{CE} were given according to the data obtained from the experiments conducted. Fig. 13 illustrates plantar flexion of the foot of one volunteer. The simulated data approach the experimental but the two lines do not coincide as well as those in Fig. 12.

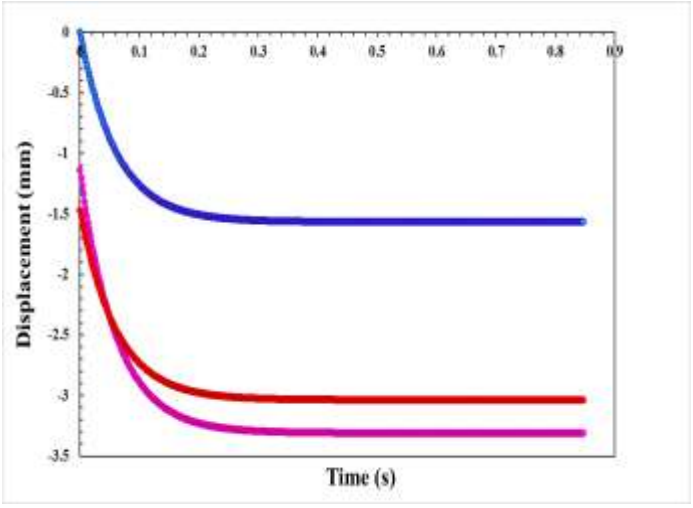

Fig. 13. Displacement over time when volunteer is plantar flexing foot. The blue line denotes the displacement x_2 over time. The magenta line symbolises the experimental data of the displacement of the muscle-tendon complex over time. The red line represents the simulated displacement of the complex when $x_1 = x_2 + C$.

5. DISCUSSION

The purpose of this study was to obtain more insight into how the muscle-tendon complex of the human gastrocnemius muscle-Achilles tendon behaves during plantar flexion, dorsiflexion and its resting position. Subsequently, a model of the complex was developed and the patterns of the movements were determined through experiments conducted in the University of Warwick Gait Laboratory and at UHCW. Assumptions were made concerning the values of the damping and spring elements of the muscle and the tendon. However, these values lie within measured values found in the literature, where the dimensions and elastic behaviour of tendinous tissue in series with the muscle fibres were studied. The values of the spring constants were assumed to lie between the ranges of 0-1000 N/m and the values of the damping factors were considered to lie between the ranges of 0-100Ns/m [9]. The geometry and architecture of the gastrocnemius muscle were determined through the ultrasounds provided by the UHCW and palpation of the legs of the volunteers before marker placement commenced, by feeling the origin and the end point of the muscle superficially. Since the soleus muscle lies underneath the Achilles tendon and cannot be felt correctly by palpation, it was omitted in this study. This will be considered in future studies.

Structural identifiability analysis of the modified Hill-type muscle model with a focus on the Achilles tendon was performed and led to show identifiable parameters that can describe the movement of the muscle-tendon complex. Parameter estimation of the model led to satisfactory agreement between measured and simulated data for the specific movements that were studied. Such a model and experimental approach offers the potential to be adapted to

other joints, such as the hip joint and the knee. The approach developed for the upper limbs [26], was proven to be suitable for the leg muscles, so we can speculate that other muscle groups can be parameterised and studied in a similar way. When investigating the nonlinear model, the solution for the quadratic equation when simulated gave a better approach to the experimental data than the simulation of the solution of the cubic equation.

This paper describes a method where tailored experiments focus on determining the characteristics of the Achilles tendon in a Hill-type muscle model. The derivation of the Achilles tendon force from the system equations for the musculoskeletal model of the Achilles tendon in section 2.2 and the implementation of that force in the muscle-tendon model in order to derive the parameters of the model as well as the nonlinear approach of the behaviour of the Achilles tendon studied through a motion capture system is, to the best of the authors knowledge, novel in the field of muscle-tendon research.

Isometric and isotonic contractions of the muscle-tendon complex are important to be examined as an initial step. Nonetheless, the way that muscles generate complex movements and behave during those complex movements is different from the way in which they behave in these specific types of contractions (isotonic, isometric). Observations and analysis of the complex movements are also necessary which will hopefully lead to a more personalised analysis of the model generated. The material properties of the gastrocnemius muscle and the Achilles tendon should also be incorporated in future studies. In addition, a spatio-temporal three-dimension description of the system would be an interesting approach to be investigated in the future.

ACKNOWLEDGEMENTS

This research project was funded by the Victoria Fernandes scholarship awarded by the School of Engineering at the University of Warwick.

REFERENCES

[1] M. R. Carmont, A. M. Highland, J. R. Rochester, E. M. Paling, and M. B. Davies, "An anatomical and radiological study of the fascia cruris and paratenon of the Achilles tendon," *Foot and Ankle Surgery*, vol. 17, pp. 186-192, 9// 2011.

[2] P. Szaro, G. Witkowski, R. Śmigielski, P. Krajewski, and B. Ciszek, "Fascicles of the adult human Achilles tendon – An anatomical study," *Annals of Anatomy - Anatomischer Anzeiger*, vol. 191, pp. 586-593, 11/20/ 2009.

[3] M. Christopher C. Nannini. (15 June). *Achilles tendon rupture*. Available: http://www.emedicinehealth.com/achilles_tendon_rupture/article_em.htm

[4] A. Saxena and D. Bareither, "Magnetic resonance and cadaveric findings of the “watershed band” of achilles tendon," *The Journal of Foot and Ankle Surgery*, vol. 40, pp. 132-136, 5// 2001.

[5] C. C. van Gils, R. H. Steed, and J. C. Page, "Torsion of the human achilles tendon," *The Journal of Foot and Ankle Surgery*, vol. 35, pp. 41-48, 1// 1996.

[6] J. H. C. Wang, "Mechanobiology of tendon," *Journal of Biomechanics*, vol. 39, pp. 1563-1582, // 2006.

[7] G. A. Lichtwark, & Wilson, A. M. , " In vivo mechanical properties of the human Achilles tendon during one-legged hopping," *Journal of Experimental Biology*, vol. 208(24), (2005).

[8] S. Malvankar and W. S. Khan, "Evolution of the Achilles tendon: The athlete's Achilles heel?," *The Foot*, vol. 21, pp. 193-197, 12// 2011.

[9] C. N. Maganaris, "Tensile properties of in vivo human tendinous tissue," *Journal of Biomechanics*, vol. 35, pp. 1019-1027, 8// 2002.

[10] C. N. Maganaris and J. P. Paul, "Tensile properties of the in vivo human gastrocnemius tendon," *Journal of Biomechanics*, vol. 35, pp. 1639-1646, 12// 2002.

[11] R. A. Zifchock and S. J. Piazza, "Investigation of the validity of modeling the Achilles tendon as having a single insertion site," *Clinical Biomechanics*, vol. 19, pp. 303-307, 3// 2004.

[12] E. Wallenböck, O. Lang, and P. Lugner, "Stress in the achilles tendon during a topple-over movement in the ankle joint," *Journal of Biomechanics*, vol. 28, pp. 1091-1101, 9// 1995.

[13] S. J. Obst, R. Newsham-West, and R. S. Barrett, "In Vivo Measurement of Human Achilles Tendon Morphology Using Freehand 3-D Ultrasound," *Ultrasound in Medicine & Biology*, vol. 40, pp. 62-70, 1// 2014.

[14] N. Chatzistefani, M. J. Chappell, C. Hutchinson, and N. D. Evans, "A Mathematical Model of the Achilles tendon in humans," *IFAC-PapersOnLine*, vol. 48, pp. 429-434, // 2015.

[15] J. Stebbins, M. Harrington, N. Thompson, A. Zavatsky, and T. Theologis, "Repeatability of a model for measuring multi-segment foot kinematics in children," *Gait & Posture*, vol. 23, pp. 401-410, 6// 2006.

[16] D. A. Winter, *Biomechanics and Motor control of Human Movement*. NJ, 2005.

[17] J. Richards, *Biomechanics in Clinic and research*, 2008.

[18] N. K. Subhra Chowdhury "Estimation of Forces and Moments of Lower Limb Joints from Kinematics Data and Inertial Properties of the Body by Using Inverse Dynamics Technique," *Journal of Rehabilitation Robotics*, pp. 93-98, 2013.

[19] D. B. Tortora Gerard J., *Principles of Anatomy & Physiology*: John Wiley and Sons, 2011.

[20] H. K. Marieb Elaine N., *Human Anatomy & Physiology*. San Fransisco: Pearson Benjamin Cummings, 2007.

[21] G. E. Robertson D., *Research Metods in Biomechanics*. USA: Edwards Brothers Malloy, 2014.

[22] T. F. Yu and A. J. Wilson, "A passive movement method for parameter estimation of a musculo-skeletal arm model incorporating a modified hill muscle model," *Computer Methods and Programs in Biomedicine,* vol. 114, pp. e46-e59, 5// 2014.

[23] A. V. Hill, "The Heat of Shortening and the Dynamic Constants of Muscle," *Proceedings of the Royal Society of London. Series B, Biological Sciences,* vol. 126, pp. 136-195, 1938.

[24] D. F. B. Haeufle, M. Günther, A. Bayer, and S. Schmitt, "Hill-type muscle model with serial damping and eccentric force–velocity relation," *Journal of Biomechanics,* vol. 47, pp. 1531-1536, 4/11/ 2014.

[25] M. F. Bobbert, P. A. Huijing, and G. J. van Ingen Schenau, "A model of the human triceps surae muscle-tendon complex applied to jumping," *Journal of Biomechanics,* vol. 19, pp. 887-898, // 1986.

[26] A. Freivalds, *Biomechanics of the upper limbs : mechanics, modeling, and musculoskeletal injuries*. USA: CRC press, 2004.

[27] A. Crowe, "A mechanical model of muscle and its application to the intrafusal fibres of the mammalian muscle spindle," *Journal of Biomechanics,* vol. 3, pp. 583-592, 1970/11/01 1970.

[28] G. L. Gottlieb and G. C. Agarwal, "Dynamic relationship between isometric muscle tension and the electromyogram in man," *Journal of Applied Physiology,* vol. 30, pp. 345-351, 1971.

[29] G. A. Lichtwark and A. M. Wilson, "Is Achilles tendon compliance optimised for maximum muscle efficiency during locomotion?," *Journal of Biomechanics,* vol. 40, pp. 1768-1775, // 2007.

[30] M. D. Mann. (2011). *Chapter 14: Muscle Contraction*. Available: http://michaeldmann.net/mann14.html

[31] D. Barrows. (2013). *The Difference Between an Isotonic and Isometric Contraction*. Available: http://www.livestrong.com/article/382348-the-difference-between-an-isotonic-and-isometric-contraction/

[32] M. J. Chappell and R. N. Gunn, "A procedure for generating locally identifiable reparameterisations of unidentifiable non-linear systems by the similarity transformation approach," *Mathematical Biosciences,* vol. 148, pp. 21-41, 2// 1998.

[33] N. D. Evans and M. J. Chappell, "Extensions to a procedure for generating locally identifiable reparameterisations of unidentifiable systems," *Mathematical Biosciences,* vol. 168, pp. 137-159, 12// 2000.

[34] C. Chillemi, A. Gigante, A. Verdenelli, M. Marinelli, S. Ulisse, A. Morgantini, *et al.*, "Percutaneous repair of achilles tendon rupture: ultrasonographical and isokinetic evaluation," *Foot and Ankle Surgery,* vol. 8, pp. 267-276, // 2002.

[35] J. J. Rankine, "(iv) Imaging of foot and ankle disorders," *Orthopaedics and Trauma,* vol. 23, pp. 412-419, 12// 2009.

[36] T. L. Switaj and F. G. O'Connor, "Chapter 43 - Gait Analysis," in *The Sports Medicine Resource Manual*, ed Philadelphia: W.B. Saunders, 2008, pp. 536-542.

[37] C. Kirtley, "Chapter 3 - Three-dimensional gait analysis," in *Clinical Gait Analysis*, C. Kirtley, Ed., ed Edinburgh: Churchill Livingstone, 2006, pp. 53-71.